Effect of molybdenum and chromium contents in sliding wear of high-chromium white cast iron: The relationship between microstructure and wear

C. Scandian [a], C. Boher [b,*], J.D.B. de Mello [c], F. Rézaï-Aria [b]

[a] Federal University of Espirito Santo (UFES), Mechanical Engineering Department CT, 29075-910 Vitória, ES, Brazil
[b] Toulouse University, Ecole Mines Albi, CROMeP, F-81013 Albi cedex, France
[c] Tribology and Materials Laboratory, Mechanical Engineering College, Federal University of Uberlândia, 38400-902 Uberlândia, MG, Brazil

Keywords:
High-chromium cast iron
Molybdenum content
Friction
Wear

A B S T R A C T

High-chromium white cast irons are commonly used in applications requiring excellent abrasion resistance, as in the mining and mineral ore processing industry. Their excellent abrasion resistance is mainly due to their solidification microstructures. During their solidification, high levels of chromium (16–32%) lead to the formation of a high-volume fraction of eutectic M_7C_3-carbides, which may or may not be associated with primary carbides in a heterogeneous austenitic/martensitic dendritic structure. Generally, in common white high-chromium cast iron, the molybdenum content is less than 3 wt.% (by weight) so as to avoid a perlitic transformation. It is reported that by addition of molybdenum in quantities of more than 3 wt.%, new carbides (M_2C, M_6C) are formed which greatly increase the high-temperature wear resistance.

In this paper, 15 high-chromium white cast alloys containing different chromium contents (16 wt.%Cr to 32 wt.%Cr) and molybdenum (Mo free to 9 wt.%Mo) are examined. For each alloy, the chemical composition and volume fraction of carbides and matrix have previously been determined. The matrix microstructure and the type of carbides depend on the relative contents of molybdenum and chromium. The wear experiments are carried out on a pin-on-disc tribometer at room temperature. The pin is made of cast iron. The wear mechanisms are observed by scanning electron microscopy (SEM). It is observed that the pin height loss, the evolution of friction versus time curves and the mean friction coefficient are largely dictated by the matrix microstructure. The carbides volume fraction and the macroscopic hardness both play only a minor role. The pin height loss is significant for a single-phased matrix and the mean friction coefficient is high. When the matrix is multiphased, the pin height loss tends towards zero and the coefficient of friction is lower. Detailed SEM observations and analysis of the evolution of the friction versus time curves indicate the substantial contribution of the large carbides in friction contact.

1. Introduction

Tabrett et al. [1] gave a range of chromium and carbon contents to define high-chromium white cast iron alloys. The respective content of these elements is between 11 to 30 wt.% for chromium and 1.8 to 3.6 wt.% for carbon. The microstructure of these alloys has been studied by several authors [1–5]. It is composed of hard primary carbides and/or eutectic carbides (M_7C_3 type) in a softer iron matrix (i.e. austenitic, martensitic, ferritic, pearlitic or bainitic). By adding the alloying elements such as molybdenum, vanadium, niobium, etc., additional carbides such as M_6C or M_2C and MC are formed. These alloys are widely used in the mining, cement, steel making and ceramic industries (crushers, pumps, sieves, etc.) that require materials with excellent abrasion resistance.

Most of the tribological research on white cast iron deals with two- or three-body abrasion resistance with a large range of chemical composition of alloying elements, under various processing conditions and heat treatments.

Generally, wear resistance is dependant on matrix microstructure, carbide types and characteristics (size, morphology, distribution, orientation [6]) as well as the volume fraction, fracture toughness and the hardness of the alloys [7–10]. It also depends on loading conditions, the features of the tribological environments, the relative movement of the contact surface and the type and size of the abrasive bodies. However, there have been only a, limited number of investigations dealing with sliding wear [11,12]. Milan et al. [12] studied HSS steel and high-chromium cast iron (HCCI) at room and high temperature, showing that, at room temperature, HSS presents a better wear resistance than HCCI.

The addition of molybdenum to a high-chromium cast iron leads to the formation of M_2C or M_6C carbides depending on the Cr/C ratio [13]. Furthermore, the molybdenum content (0.5–3 wt.%) pre-

* Corresponding author. Tel.: +33 563493169; fax: +33 563493099.
E-mail address: christine.boher@enstimac.fr (C. Boher).

vents the perlitic transformation of the austenite and increases the hardenability [1,2] of alloyed cast irons. A molybdenum content greater than 3 wt.% could improve high-temperature wear resistance. Ikeda et al. [11] have performed sliding wear experiments on a cast iron with a ratio Cr/C of 5. It is shown that by adding molybdenum, M_2C carbides are formed which contribute to enhancing high temperature abrasion resistances.

The general purpose of this study is to investigate the room- and high-temperature wear resistances of experimental white cast irons with high-chromium and high-molybdenum contents and a Cr/C ratio of 10 [13]. However, this contribution deals exclusively with the room-temperature results.

The Cr/C ratio of 10 leads to the formation of M_6C carbides instead of M_2C carbides [13]. To study the contribution of M_6C carbides on the high-temperature wear resistance of these alloys, tribological tests were carried out by using a high temperature pin-on-disc tribometer in sliding wear conditions. More precisely, as an initial approach, the aim of this paper is to study and compare the tribological behaviour, in sliding wear, of these different experimental white cast irons at room temperature.

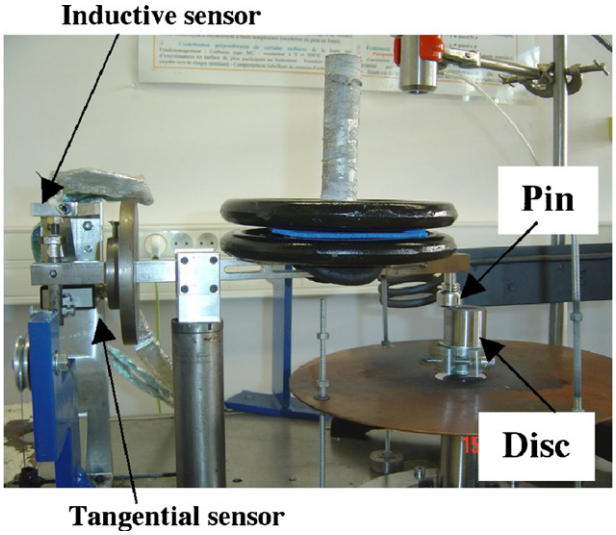

Fig. 1. General view of the pin-on-disc tribometer.

2. Experimental procedure and materials

2.1. Experimental procedure

Friction tests are carried out on a pin on disc tribometer in dry conditions (Fig. 1) [14,15]. The discs are 35 mm in diameter and 40 mm thick. They have a continuous rotating movement and the rotating speed can vary from 30 to 3000 rpm (Fig. 2a). The pin has a cylindrical shape (10 mm in diameter, 16 mm in length) with a truncated conic end with a flat circular surface of 2 mm in diameter (contact surface) (Fig. 2b). Before any test, the pin and the disc are first polished down to 1200 grades and then cleaned by acetone and ethanol using ultrasound. Normal loading is carried out by dead weights. The tangential forces (friction) are measured using a strain gauge located in the friction plane. A Kaman inductive sensor (±500 μm), located at the extremity of the pin arm, could measure the total wear-loss values (a combination of the pin height loss and depth of the disc wear track).

The friction forces and the total wear loss values are directly recorded during the friction test using software developed on LABVIEW. The data sampling rate is 10 Hz.

Table 1
Friction experimental conditions.

Sliding speed	Normal load	Test duration	Ambient
0.3 m/s	20 N	1800 s	Room temperature

The pin height loss (h) is calculated from the variation between the initial diameter of the contact surface (Di) and its final diameter (Df) (Eq. (1)). All diameters are measured by optical microscopy.

$$h = \frac{Di - Df}{2} \tag{1}$$

2.2. Set-up conditions

All friction experiments are carried out under the same testing conditions (Table 1). Each friction test is carried out twice for repeatability considerations.

The worn surfaces are examined by optical microscopy, and the cross-sections (along the friction direction) by scanning electronic microscopy and dispersive energy analysis.

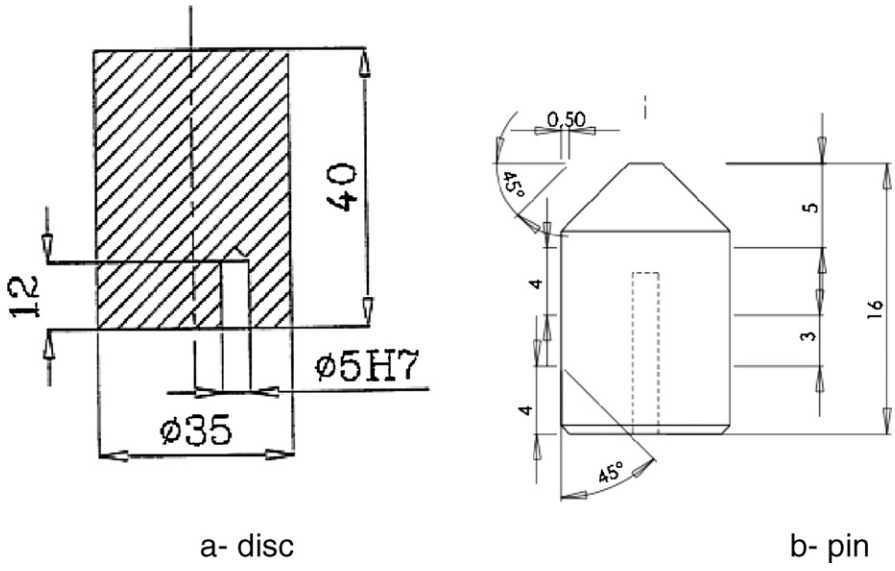

Fig. 2. Schemata of the tribological pin and disc.

Table 2
Microstructure of different white cast irons as a function of chromium and molybdenum contents (wt.%).

Mo (wt.%)	Cr (wt.%)			
	16	24	28	32
0	Hypoeutectic alloy, matrix: α; carbides: M_7C_3	Hypoeutectic alloy, matrix: α/α′; carbides: M_7C_3	Eutectic alloy, matrix: α; carbides: M_7C_3	Hypoeutectic alloy, matrix: α; carbides: M_7C_3
3	Hypoeutectic alloy, matrix: α/α′/γ; carbides: $M_7C_3 + M_6C$	Hypoeutectic alloy, matrix: α/α′/γ; carbides: $M_7C_3 + M_6C$	Eutectic alloy ⇒ As-hypereutectic alloy, matrix: α; carbides: $M_7C_3 + M_6C$	Hypereutectic alloy, matrix: α; carbides: $M_7C_3 + M_6C$
6				
9		Hypoeutectic alloy, matrix: α; carbides: $M_7C_3 + M_6C$		

Topographies of the worn surface of pins and discs are carried out with a quasi-confocal ALTISURF® microscope with extended *z*-axis field using Halogen as a light source. Field extension is obtained by spectral coding of the *z*-axis. The surface topology is reconstructed by contact-less 3D (*x*-*y*-*z*) probe scanning. The resolution of the probe depends on the depth of the field in a range between 1 nm and 300 nm. The measurements are performed with a 350 μm probe providing *z*-axis resolution of 11 nm. The scanning advance step (*x*, *y*) is 5 μm. The (*x*, *y*) area of the 3D surfaces of the disc tracks is 5 mm × 5 mm. The size of the topography area of the pin surface is optimised in order to obtain the image of the whole 3D-surface of the pin. All the 3D disc surfaces and 3D pin surfaces are processed by the roughness analysis software ALTIMAP®. This method is widely used to measure the depth of the disc wear track.

2.3. Materials

The disc material is a low-carbon perlito-ferritic steel, AISI 1018. Pins are composed of white cast irons with different high-chromium and high-molybdenum contents. The chromium/carbon ratio is always 10. Samples are first sand cast and natural air-cooled. Prismatic samples (40 mm × 40 mm × 70 mm) are removed from the as-cast samples. Then tribological pins are machined from these samples. Four white cast iron groups have been studied:

- Two groups are hypoeutectic alloys (16 and 24 wt.% chromium).
- One group is an eutectic alloy (28 wt.%Cr).
- One group is a hypereutectic alloy (32 wt.%Cr).

For each group, four alloys with different Mo content (0, 3, 6 and 9 wt.%) are investigated. Fifteen specimens have been prepared and tested (Table 2) (the 28 wt.%Cr–6 wt.%Mo sample was not studied).

The microstructure of the Mo-free hypoeutectic alloys with 16 wt.%Cr, consists of a dendritic ferritic matrix (Feα) with inter-dendritic Maratray pearlite (α + M_7C_3 carbides) [2,13] surrounded by small interdendritic as well as eutectic M_7C_3 carbides (Fig. 3a). According to the equilibrium phase diagram, the matrix should be austenitic and not ferritic. This phase modification is relevant to the die-casting cooling process.

With Mo-free and 24 wt.%Cr, the microstructure looks the same as that described above because it is still dendritic but composed of α/α′ (ferritic and martensitic).

For Mo-free and 28 wt.%Cr (eutectic alloys group) the microstructure consists of more or less mixed strips of α and M_7C_3 carbides. The carbide size is about 10–20 μm (Fig. 3b).

For Mo-free and 32 wt.%Cr (hypereutectic alloy group), the large primary carbides capture a considerable amount of carbon content. The matrix is ferritic due to the slow cooling rate of the cast (Fig. 3c).

The Mo-addition in hypoeutectic alloys impedes the austenitic transformation into pearlite, and facilitates the formation of a martensite microstructure, thus increasing hardenability of the alloy (Table 2). For hypoeutectic alloys, three different phases are present in the matrix dendrites (ferrite α/martensite α′/austenite γ). The amount of inter-dendritic M_7C_3 carbides increases with dendrite size enhancements. New eutectic carbides (M_6C carbides) coarsened because molybdenum is a carburising element.

The Mo alters the Cr–C equilibrium and modifies the phase diagram domains in eutectic and hypereutectic alloys, which strongly influences the alloy microstructure:

- The as-known eutectic alloy (28 wt.%Cr) becomes a hypereutectic type alloy with primary M_7C_3 carbides, M_6C carbides and a ferritic matrix.
- The as-known hypereutectic alloy (32 wt.%Cr) keeps the primary M_7C_3 carbides with a ferritic matrix microstructure and develops M_6C carbides.

The bulk Vickers hardness of pins (HV10) as a function of chromium and molybdenum contents is given in Fig. 4. For an equivalent chromium weight percentage, when the molybdenum content increases, the hardness is enhanced. The bulk hardness of hypoeutectic alloys can reach 700 (HV10). By addition of Mo, new M_6C carbides are formed and the matrix is transformed from a single-phase (α) to a multiphase (α/α′/γ). Such a modification is not observed in 24 wt.%Cr with 9 wt.%Mo because the addition of Mo changes the phase equilibrium diagram to a ferritic matrix and therefore the hardness decreases.

The eutectic M_6C carbides, rich in Mo with a "fishbone" microstructure, are closely linked (embedded) in a matrix phase.

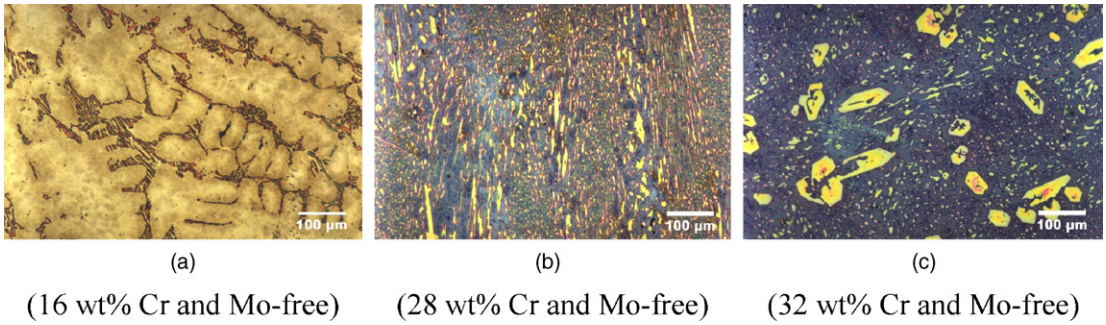

Fig. 3. Typical microstructures of the different groups of alloys: (a) hypoeutectic alloys; (b) eutectic alloys; (c) hypereutectic alloys [13].

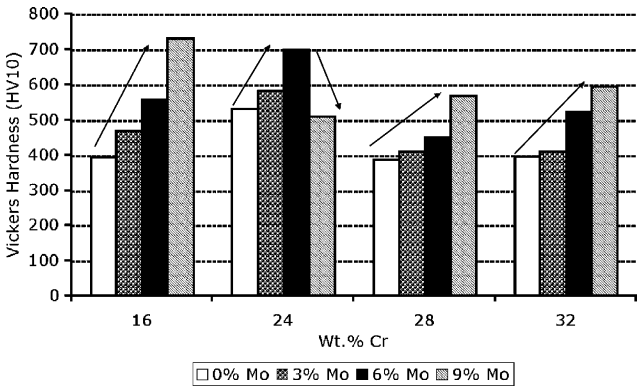

Fig. 4. Macro Vickers hardness (HV10) of the different alloys as a function of chromium and molybdenum contents (wt.%).

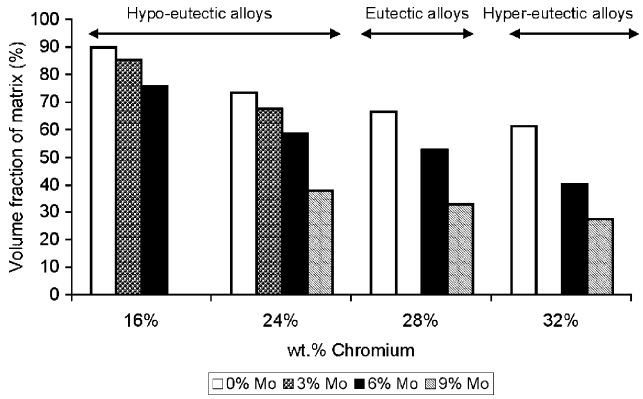

Fig. 5. Volume fraction of matrix (%) in the different alloys as a function of chromium and molybdenum contents (wt.%).

Even if hard and large M_7C_3 carbides (eutectic and primary) are formed, the hardness of eutectic or hypereutectic alloys is slightly lower than the previous ones, for a same amount of Mo content, because the matrix remains in the ferritic phase.

The volume fraction of the matrix is determined by image analysis [13]. The volume fraction of the matrix decreases with an increase in the content of the alloying elements chromium and molybdenum, since M_7C_3 and M_6C eutectic carbides are formed, as well as M_7C_3 primary carbides. The matrix fraction is always greater than 40% for hypoeutectic alloys regardless of the wt.%Mo (Fig. 5).

3. Results and discussion

3.1. Role of the microstructure on wear results

The evolution of the pin height loss by wear as a function of chromium and molybdenum contents is reported in Fig. 6. Regardless of the chromium and molybdenum contents (wt.%), when the matrix microstructure is fully ferritic, the values of pin height loss are the highest (Fig. 6). When the matrix microstructure is multiphased (α/α' or $\alpha/\alpha'/\gamma$), the values of pin height loss decrease considerably and could be close to zero, whatever the Cr or Mo content (wt.%) may be. For a given Cr content, the pin height loss is dependent on the bulk hardness and on the Mo content (wt.%) and when the bulk hardness increases, the pin height loss decreases. However, for the same level of bulk hardness (e.g. 24 wt.%Cr–3 wt.%Mo—Fig. 6b and 32 wt.%Cr–9 wt.%Mo—Fig. 6d), the pin height losses are not equivalent. The pin height loss is always higher when the matrix is ferritic (32 wt.%Cr–9 wt.%Mo—Fig. 6d). These observations lead to the conclusion that the matrix microstructure is a more pertinent parameter to control wear loss than bulk hardness.

When Mo content increases, the matrix of hypoeutectic alloys (16 wt.%Cr, 24 wt.%Cr) is multiphased, Mo-rich carbides (M_6C type) appear and the pin height loss is low (16 wt.%Cr–3 wt.%Mo–24 wt.%Cr–3 wt.%Mo) (Fig. 6b) and could be close to zero (16 wt.%Cr–6 wt.%Mo–24 wt.%Cr–6 wt.%Mo—Fig. 6c

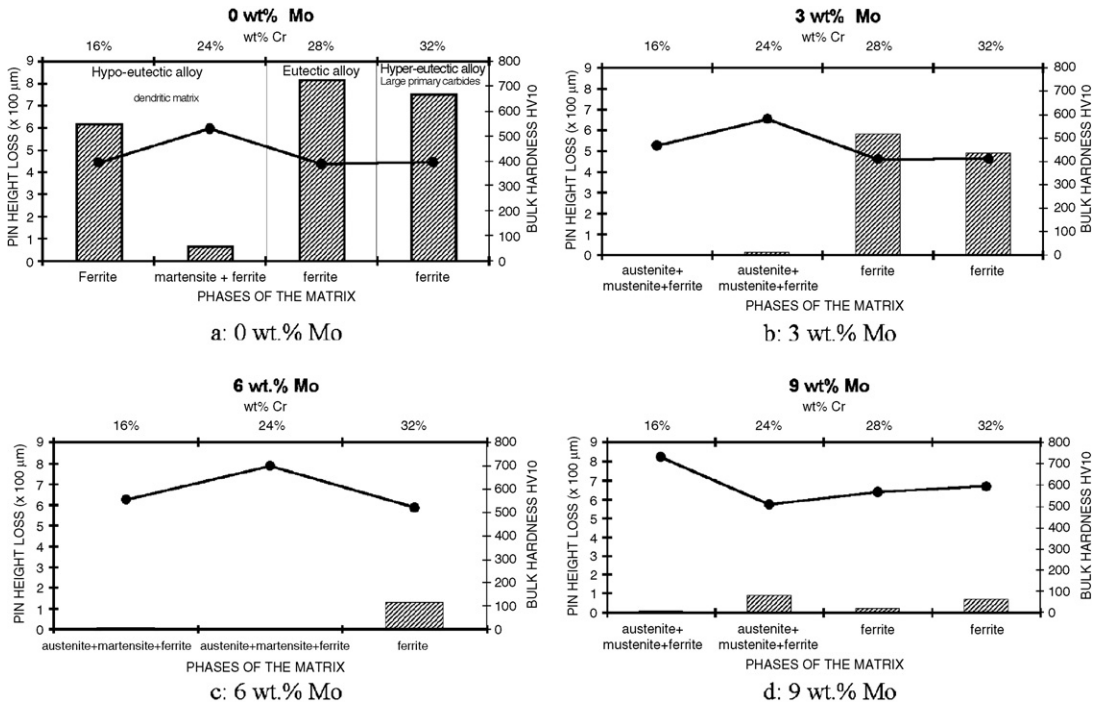

Fig. 6. Pin height loss "h" (hachured rectangles) and bulk hardness of the alloys (full lines) as a function of Cr and Mo (wt.%) in relative matrix microstructures (a: 0 wt.%Mo; b: 3 wt.%Mo; c: 6 wt.%Mo; d: 9 wt.%Mo).

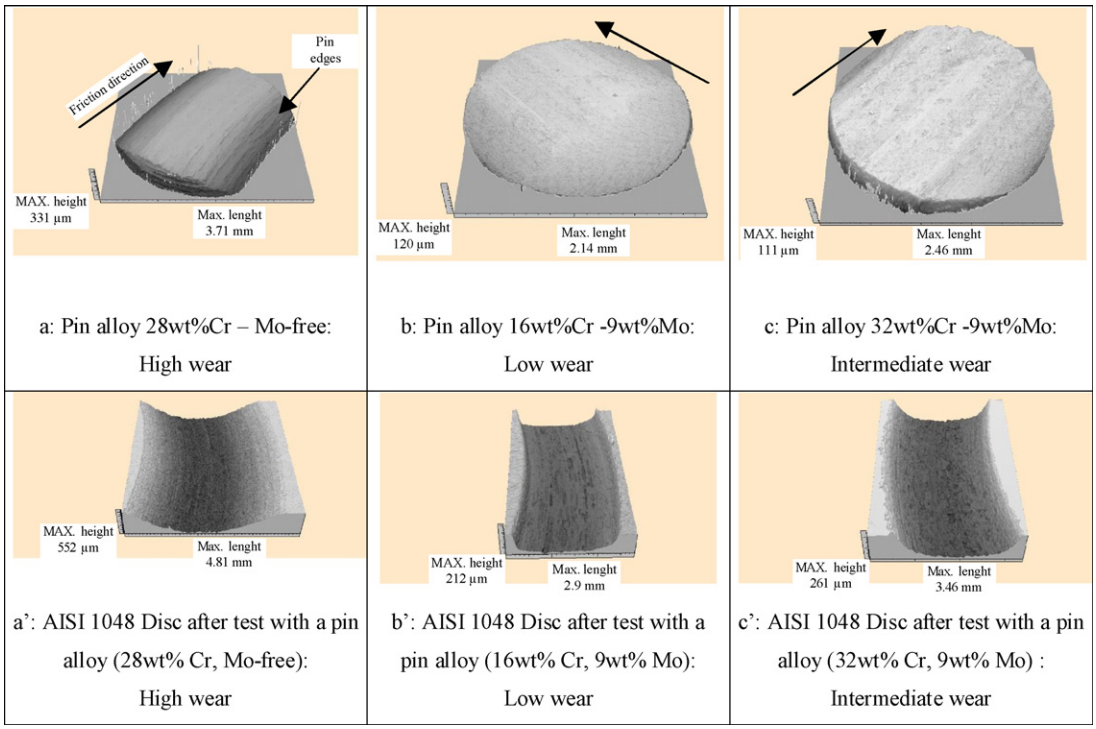

Fig. 7. Topographies of the 3D surfaces of the pin (above: a; b; c) and a portion of the counter-face disc wear track (below: a′; b′; c′). The black arrows indicate the sliding directions.

16 wt.%Cr–9 wt.%Mo—Fig. 6d). As the volume fraction of the matrix falls, the carbides fraction rises, and thus the pin height loss decreases because the global hardness increases due partly to the contribution of M_6C carbides but mainly to the strengthening of the matrix by solid solution alloying. In addition, the involvement of M_6C carbides also favours the wear resistance.

The special behaviour of the 24 wt.%Cr–9 wt.%Mo alloy (Fig. 6d) is significant. Initially the 24 wt.%Cr has a hypoeutectic chemical composition with a multiphased (α/α') matrix. For low Mo contents (3 wt.% and 6 wt.%Mo), the matrix microstructure is always multiphased ($\alpha/\alpha'/\gamma$), and the volume fraction of carbides increases and the quantity of M_6C carbides grows. In this case, the pin height loss is very low (close to zero). For high content Mo alloys (9 wt.%), the phase equilibrium is shifted towards the ferritic-dominant domain [13]. The bulk hardness falls and the pin height loss increases. The volume fraction of carbides does not prevent wear.

The eutectics alloys (28 wt.%Cr), as well as the hypereutectic alloys (32 wt.%Cr), keep a ferritic matrix regardless of the Mo content. The large M_7C_3 carbides and the enhancement of M_6C carbides favour the wear resistance but the pin height loss is not close to 0 (Fig. 6c and d).

These wear results assume that the matrix microstructure plays an important role in wear loss. A ferritic matrix with a dendritic microstructure and eutectic M_7C_3 carbides (e.g. 16 wt.%Cr–Mo-free) seems to be more resistant to shear stresses than a ferritic matrix with a more "lamellar" microstructure and eutectic or primary M_7C_3 carbides (Mo-free and 24 wt.%Cr or 32 wt.%Cr). The same result is observed with a ferritic matrix with a dendritic microstructure and eutectic M_7C_3 and M_6C carbides (24 wt.%Cr–9 wt.%Mo) in comparison with a ferritic matrix with primary M_7C_3 carbides and eutectic M_6C carbides (32 wt.%Cr–9 wt.%Mo) (Fig. 6d).

The topography measurements of the pins clearly reveal the different pin wear morphologies. Considering the scale of roughness measurements, for pins with a single-phased ferritic matrix and eutectic or primary M_7C_3 carbides, the diameter of the wear surface of the pin is greater than the initial diameter and the pin surface loses its flat feature to take on a bowed shape (Fig. 7a). Thus, the shape of the wear track of the disc self-adjusts to be in good conformity with its counter-face (Fig. 7a′). The edges of the pin friction surface sliding "parallel" to the rotation direction are more easily worn because they are the regions of high stresses (friction between the walls of the disc wear track and the pin edges). For the flat pins, the Hertz maximum pressure is located on the pin perimeter. The Hertz pressure could also explain the bowed shape of the pin. The depth of the disc wear track is also high (>400 µm). The friction contact is established between two ferritic materials. Examinations of cross-sections of the pin (28 wt.%Cr–Mo-free) (Fig. 8) show that pin debris is constituted of matrix particles and, in a lesser proportion, fragments of the large M_7C_3 carbides broken under shear stresses. Large M_7C_3 eutectic carbides are brittle and very sensitive to friction

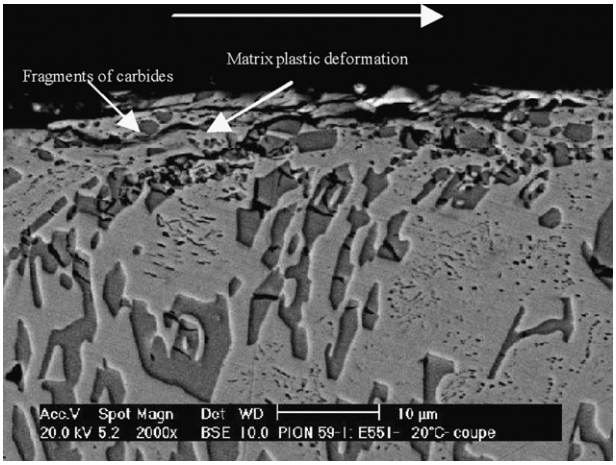

Fig. 8. Examination of the pin cross-section (28 wt.%Cr–0 wt.%Mo). Ferritic matrix with eutectic M_7C_3 carbides. The white arrow indicates the sliding direction.

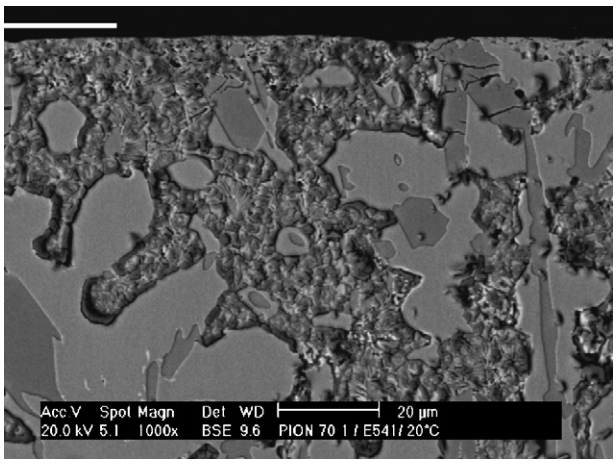

Fig. 9. Examination of the pin cross-section (32 wt.%Cr–3 wt.%Mo). Ferritic matrix with primary M_7C_3 carbides and eutectic M_6C carbides. The white arrow indicates the sliding direction.

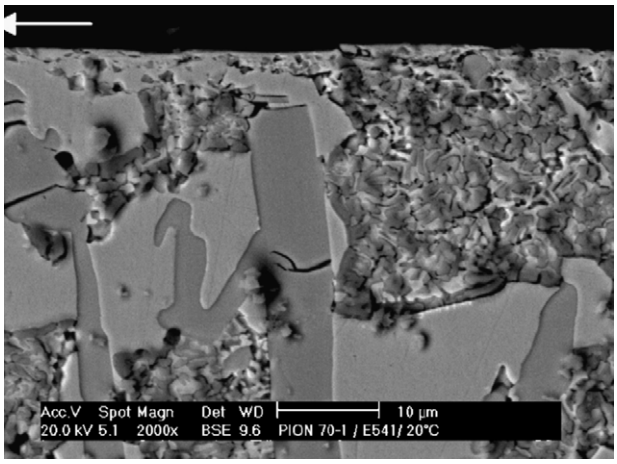

Fig. 11. Examination of the pin cross-section (32 wt.%Cr–6 wt.%Mo). Single-phased matrix with primary M_7C_3 carbides and eutectic M_6C carbides. The white arrow indicates the sliding direction.

forces, showing a lot of micro-cracks. In addition, the plastic deformation of the matrix, at pin subsurface, contributes to the carbide debris formation (Fig. 8).

For higher Cr and Mo contents (32 wt.%Cr–3 wt.%Mo), the eutectic M_6C carbides are tightly embedded in a matrix phase (Fig. 9). Contrary to the M_7C_3 carbides, these M_6C carbides do not present micro-cracks, but considering that they are mixed in a ductile phase, a very low plastic deformation is observed. Therefore, it is supposed that they contribute to improving the wear resistance and are not removed from the contact zone as debris. They act as a network to strengthen the shear resistance of the alloy.

The disc and pin debris are significantly involved in the friction contact and contributes to the wear of the two counter-faces.

For alloys with a multiphased matrix, the pin surface keeps its initial flat feature since its wear is very low (Fig. 7b). The shape of the disc wear track is also in good conformity with the pin shape (Fig. 7b′). Examinations of cross-sections of the pin (24 wt.%Cr–6 wt.%Mo) (Fig. 10) show some micro-cracks of the M_7C_3 carbides and no plastic deformation of the multiphased matrix.

For alloys with a single-phased matrix and large primary M_7C_3 carbides, the final shape is slightly bowed (Fig. 7c–c′) because there is an intermediate level of wear. The pin cross-section (32 wt.%Cr–6 wt.%Mo) (Fig. 11) always shows micro-cracks of M_7C_3

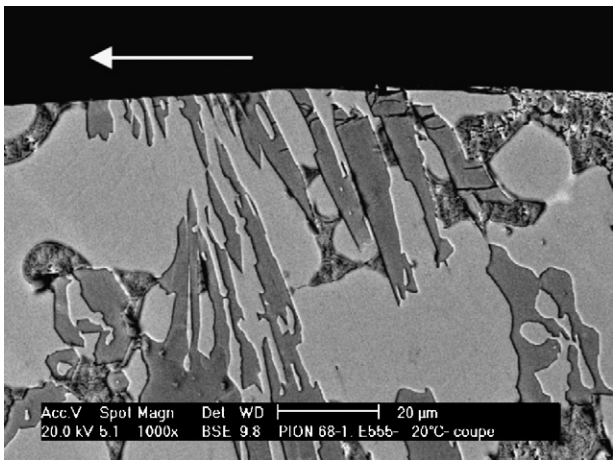

Fig. 10. Examination of the pin cross-section (24 wt.%Cr–6 wt.%Mo). Multiphased matrix with eutectic M_7C_3 carbides and eutectic M_6C carbides. The white arrow indicates the sliding direction.

and a very low plastic deformation of the matrix at the extreme surface.

The pin surface evolution is also studied through the evolution of the Sa value (µm), which is the arithmetic mean deviation of the surface directly measured from worn surface without any filtering operations (without cut-off). The higher the Sa value, the more the pin loses its initial shape. The initial value of Sa (mean value measured from all the pins) is 8 ± 2 µm. The values of "Sa" greatly superior to 8 are assigned to ferritic matrix alloys (Fig. 12). The values of "Sa" close to 8 are obtained for multiphased matrix alloys or when the wear loss is very low. The values of Sa are in good agreement with pin height loss tendencies.

3.2. Friction results

Fig. 13 illustrates the general aspect of the evolution of friction coefficient versus test duration and it is representative of all tests. Two significant trends are observed:

For alloys with a single-phased matrix and a high matrix volume fraction (>60%), the mean friction coefficient "μ" is higher than 0.7. The evolution of the friction coefficient versus test duration is mainly constant but displays two stages (Fig. 13). At the beginning of the friction test, the amplitudes of the fluctuations of the friction coefficient values are large ($0.6 < \mu < 1.1$). The high values and large fluctuations of the friction coefficient confirm that the matrix is a rather ductile or soft type material. Following this stage, the

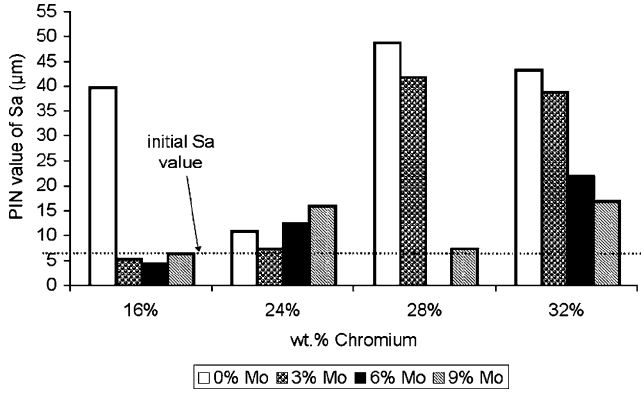

Fig. 12. Value of the arithmetic mean deviation of the surface "Sa" (µm), from the 3D surface, versus Cr and Mo contents.

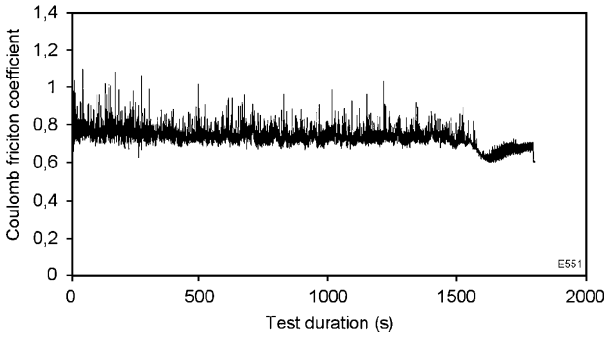

Fig. 13. Evolution of friction coefficient with test time (28 wt.%Cr–Mo-free).

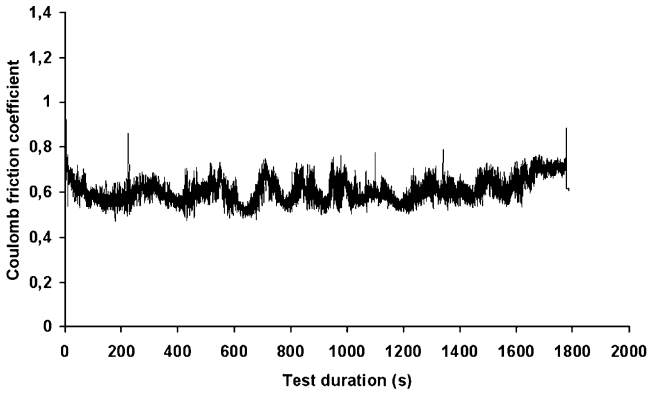

Fig. 15. Friction coefficient versus test duration (24 wt.%Cr–3 wt.%Mo).

amplitude of the friction fluctuations decreases significantly in the second stage.

For the same chromium content (hypereutectic alloys: 32 wt.%Cr), the duration of the first stage is dependent on the volume fraction of carbides (Fig. 14). When the Mo content increases, the M_6C carbides volume fraction increases as does the bulk hardness; the volume fraction of M_7C_3 carbides stays unchanged but their size increases enormously [13].

As of today, the two main hypothesis, we can develop for the break in the friction evolution for a single-phased matrix alloy is a modification of the ferritic matrix and a third layer made up of debris which could occurs in the contact. The plastic deformation of the matrix could increase its local hardness and lead to this behaviour. In addition, the lower the volume fraction of the matrix (or the higher the volume fraction of the carbides) the shorter is the time in which the modification of the evolution of the friction coefficient happens. A third body layer could made up of debris could accommodate the friction evolution. In the two cases, more investigations are to be carried out.

For alloys with a multiphased matrix, the friction curves versus test duration are different (Fig. 15). They are no longer regular but display large variations during the test. The mean value of the friction coefficient is a little lower than 0.7 (24 wt.%Cr–Mo-free; 24 wt.%Cr–3 wt.%Mo; 24 wt.%Cr–6 wt.%Mo). In this case, it should be noted that even if the friction coefficient is high, the wear loss of the pin is very low.

4. Conclusions

Room temperature and sliding wear behaviour of experimental white cast irons with various contents of chromium (16 wt.%, 24 wt.%, 28 wt.% and 32 wt.%) and molybdenum (0 wt.%, 3 wt.%, 6 wt.% and 9 wt.%) were investigated.

The wear results highlight that the microstructure of the matrix displays a strong influence on sliding wear resistance: when the matrix is ferritic single-phased, regardless of the Mo content, pin wear loss is significant. When the matrix is multiphased ($\alpha/\alpha'/\gamma$), the wear loss tends towards zero. Another point is that matrix microstructure is more significant in dictating wear loss than bulk hardness. In fact, bulk hardness is less relevant as a wear control parameter. For the same Cr content and a single-phased matrix, the hardness increases with Mo content and the wear loss decreases.

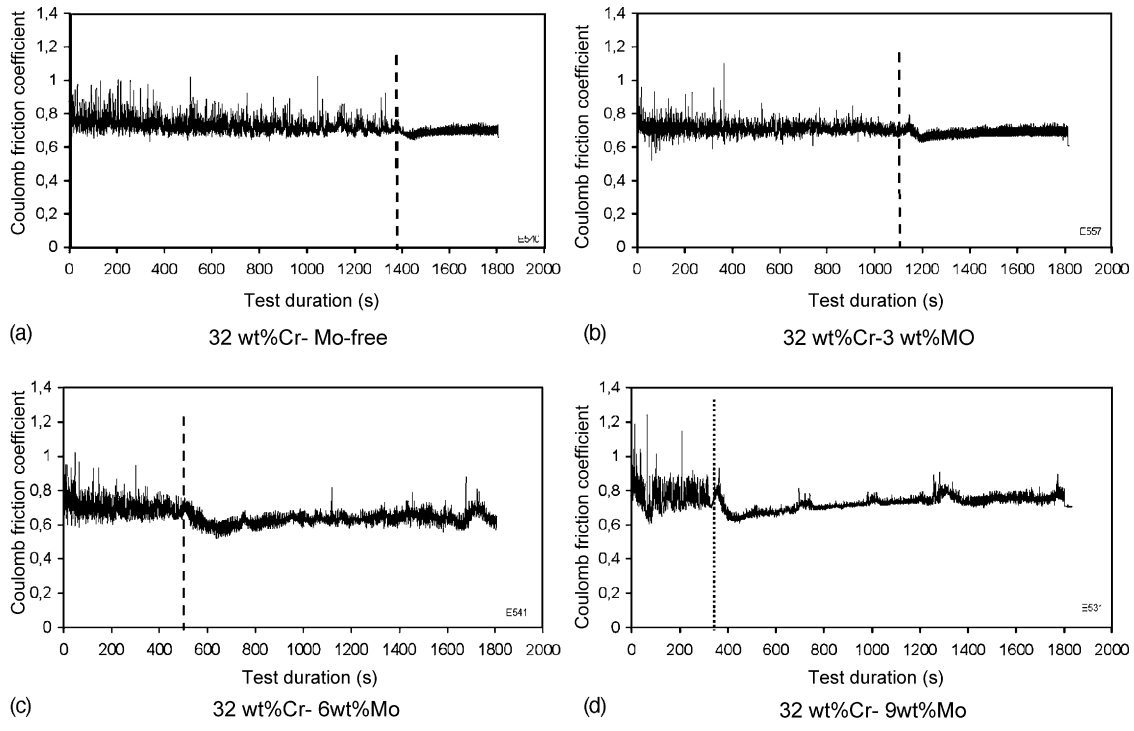

Fig. 14. Friction coefficient versus test duration (32 wt.%Cr): diminution of the first stage of the friction (a: 32 wt.%Cr; b: 32 wt.%Cr–6 wt.%Mo; c: 32 wt.%Cr–6 wt.%Mo; d: 32 wt.%Cr–9 wt.%Mo).

But for an equivalent level of hardness, the wear loss is always higher when the matrix is strictly ferritic. In addition, the ferritic matrix can be more easily plastically deformed under frictional tangential forces and the plastic deformation of the matrix contributes to the carbide micro-cracks and debris formation.

Micro-cracks are always clearly observed with eutectic or primary M_7C_3 carbides but never with M_6C (at the level of measurement resolutions used). These last carbides seem to contribute much better to enhancing the wear resistance of the alloy.

The friction results are also very interesting. For a single-phased matrix, the friction curves display two stages. First, there is a stage with high amplitudes of fluctuations in the friction coefficient and a high average friction and, after this stage, a second stage with low fluctuation amplitudes. This result is very significant with 32 wt.%Cr, where the duration of the first stage decreases with the Mo content. For a multiphased matrix, the friction curves do not display the same behaviour.

Acknowledgements

The authors would like to acknowledge the technical assistance and contributions of S. Leroux and S. Tovar from the Ecole des Mines, Albi.

References

[1] C.P. Tabrett, I.R. Sare, M.R. Ghomaschil, International Materials Reviews 41 (1996) 59–80.
[2] F. Maratray, R. Usseglio-Nanot, Facteur Affectant la Structure des Fontes Blanches au Chrome et au Molybdène, 1ed Paris, France, Climax Molybdenum, 1970, pp. 5–32.
[3] L.F. Powell, L.S. Heard, Proceedings of the 34th Conference Australian Institute of Metal, 1981, pp. 58–62.
[4] J.D.B. De Mello, M. Durrand-Charre, M.S. Hamar-Thibault, Metallurgical Transactions A 14A (1983) 1793–1801.
[5] O.N. Dogan, J.A. Hawk, G. Laird II, Metallurgical and Materials Transaction A 28A (1997) 1315–1328.
[6] O.N. Dogan, J.A. Hawk, Wear 189 (1995) 136–142.
[7] K.H. Zum Ghar, G.T. Eldis, Wear 64 (1980) 175–194.
[8] K.H. Zum Ghar, Tribology International 31 (1998) 587–596.
[9] H. Berns, Wear 254 (2003) 47–54.
[10] C. Cetinkaya, Materials & Design 27 (2006) 437–445.
[11] M. Ikeda, T. Umeda, C.P. Tong, T. Suzuki, N. Niwa, O. Kato, ISIJ International 32 (1992) 1157–1162.
[12] J.C.G. Milan, M.A. Carvalho, R.R. Xavier, S.D. Franco, J.D.B. De Mello, Wear 259 (2005) 412–423.
[13] S.M. Carvalho, M.C.S. Macêdo, J.D.B. Mello, C. Scandian, Materials Characterization (2008).
[14] C. Vergne, C. Boher, R. Gras, Wear 250 (2001) 322–333.
[15] O. Barrau, C. Boher, R. Gras, F. Rézaï-Aria, Wear 263 (2007) 160–168.